Proceedings of the XII Serbian-Bulgarian Astronomical Conference (XII SBAC) Sokobanja, Serbia, September 25-29, 2020
Editors: L. Č. Popović, V. A. Srećković, M. S. Dimitrijević and A. Kovačević
Publ. Astron. Soc. "Rudjer Bošković" No 20, 2020, 23-31

COLOR VARIABILITY OF SOME QUASARS IMPORTANT TO THE ICRF – GAIA CRF LINK

MILJANA D. JOVANOVIĆ, GORAN DAMLJANOVIĆ,
ZORICA CVETKOVIĆ, RADE PAVLOVIĆ and MILAN STOJANOVIĆ

Astronomical Observatory, Volgina 7, 11060 Belgrade, Serbia
E-mail: miljana@aob.rs, gdamljanovic@aob.rs,
zorica@aob.rs, rpavlovic@aob.rs, mstojanovic@aob.rs

Abstract. The International Celestial Reference Frame (ICRF) and Gaia CRF will be two reference frames with similar precision. To link ICRF provided with very long baseline interferometry (VLBI) in radio and Gaia CRF in optical wavelength is necessary to observe and monitor set of objects visible in both wavelengths. Observations of 47 candidate sources important for the link have been carried out by using two telescopes located at the Astronomical Station Vidojevica (of the Astronomical Observatory of Belgrade) and the one at the Rozhen National Astronomical Observatory (Bulgaria). The brightness variability (V and R bands) of five candidate sources was tested using the F-test. The color variability for the period from July 2016 to August 2019 for these five objects, and color magnitude dependences for the same period are presented in this paper.

1. INTRODUCTION

The third data realization of the International Celestial Reference Frame (ICRF3) was adopted by the International Astronomical Union (IAU) in August 2018 (Charlot et al. 2020). The ICRF3 is based on data obtained for about 40 years at radio frequencies (8.4 and 2.3 GHz) and data collected for the past 15 years at higher radio frequencies (24 GHz and dual-frequency 32 and 8.4 GHz) by very long baseline interferometry (VLBI).

The early third Gaia data release (Gaia EDR3) should be available from 3 December 2020, two years before the full data release. The Gaia EDR3 will contain data of about 1.8 billion sources and provide full astrometric information (positions, parallaxes, and proper motions) for about 1.5 billion sources. The currently available, second Gaia data release (Gaia DR2), published on 25 April 2018, provides celestial positions and G magnitudes for about 1.7 billion sources and provide positions, parallaxes, and proper motions for about 1.3 billion sources

(Gaia Collaboration et al. 2018). To link the Gaia CRF (based on the observations at optical wavelength) with the ICRF (based on the VLBI observations at radio wavelengths) it is required to observe a set of quasars (QSOs) visible in the optical domain. For this link are suitable only 10% of ICRF sources (about 70 sources). We observed the 47 candidates sources for this link with high astrometric quality (Bourda et al. 2011) since July 2016. These sources are Active Galactic Nuclei (AGNs), mostly QSO, the others are BL Lacertae – BL Lac and Seyfert galaxies type 1. The one of properties of AGNs is flux variability at different wavelength. These variations are divided into three classes (Gupta 2014): Intra Day Variabilities (those of less than a day), Short Term Variability (within the range of a few days to a few months), and Long Term Variability (from a few months to several years). It is necessary to monitor brightness variability of candidate sources for the link between two reference frames over a longer period of time.

The subject of this paper is investigation of color variability of five AGNs which have been the most observed objects. The results of investigation of the brightness variability of these five sources for a similar period of time are presented in papers: Jovanović (2019), and Jovanović and Damljanović (2020). The object properties are listed in Table 1: the coordinates are taken from SDSS DR14, the redshift (*z*) is from the NASA/IPAC Extragalactic Database – NED (https://ned.ipac.caltech.edu/), and the type is from SIMBAD Astronomical Database.

Table 1: The main properties of objects.

Object	$\alpha_{J2000.0}(^o)$	$\delta_{J2000.0}(^o)$	z	Type	Observation date (mmddyyyy)		No. of observations per filter
					start	finish	V, R
1535+231	234.31041	23.01126	0.462524	QSO	07022016	08062019	20, 24
1556+335	239.72993	33.38851	1.653476	QSO	07022016	08062019	20, 27
1607+604	242.08560	60.30783	0.178000	BL Lac	07022016	08062019	23, 27
1722+119	261.26810	11.87096	0.018000	BL Lac	07022016	08082019	22, 26
1741+597	265.63334	59.75186	0.400000	BL Lac	07042016	08072019	34, 40

2. OBSERVATIONS AND PHOTOMETRY

The observations were made using three different telescopes. Two telescopes are located at Astronomical Station Vidojevica (ASV) of the Astronomical Observatory of Belgrade and third one is located at the Rozhen NAO in Bulgaria. The details about used telescopes (ASV with mirror diameter 60 cm and 1.4m, and Rozhen 2m) and mounted CCD cameras are presented in paper Jovanović (2019). Every nights two CCD images per V and R filter have been obtained and bias, dark and flat frames which were used for reduction of CCD images. The reduction and corrections (for bad pixels and cosmic rays) were done by using Image Reduction and Analysis Facility – the IRAF scripting language (ascl:9911.002) (Tody 1986, 1993).

The brightness of objects was determined using differential photometry with two comparison stars with similar brightness and color to that of the object. In the same manner, the brightness of a few control stars was determined for the every observing night. The (comparison and control) stars are located in the object vicinity. The stars were chosen from the Sloan Digital Sky Survey Data Release 14 (SDSS DR14) catalogue (Abolfathi et al. 2018), except for the object 1722+119 they are chosen from the set of stars proposed in paper Doroshenko et al. (2014). We selected stars following several criteria. Out of the stars in the objects vicinity, we chose stars which are not variable, not too bright or faint stars (with g, r and i magnitudes outside the range 14.5 – 19.5) or not very blue or red (outside the ranges 0.08 < r-i < 0.5 and 0.2 < g-r < 1.4), etc.

The transformation from the PSF g, r, and i magnitudes from the SDSS DR14 catalogue to the Johnson-Cousins V and R ones, was performed using equations (Chonis and Gaskel 2008):

$$V = g - (0.587 \pm 0.022)(g - r) - (0.011 \pm 0.013)$$
$$R = r - (0.272 \pm 0.092)(r - i) - (0.159 \pm 0.022).$$

The V and R magnitudes of the stars for the 1722+119 object are taken from the paper Doroshenko et al. (2014). In the Table 2. are listed coordinates of objects and their two comparison (A and B) and control stars, the V_C and R_C magnitudes of stars (obtained using mentioned equations for stars from SDSS DR14, and those from Doroshenko et al. (2014)), along with V_O and R_O (calculated magnitudes using differential photometry) of the objects and stars.

The presented objects were observed for about three years. During this period, brightness of two objects, 1722+119 and 1741+597, changed about 2.0 and 1.7 magnitudes in both filters, respectively. The brightness of these two objects has the higher standard deviation. The object 1722+119 has standard deviation around 0.6 mag and 1741+597 around 0.4 mag per filter. The light curve of R magnitude of object 1722+119 with light curves of its comparison and control stars is presented in Figure 1. The brightness of 1535+231 and 1607+604 had changes about 0.6 and 0.4 magnitudes in both filters, respectively. The standard deviations are around 0.2 and 0.1, per filter, respectively. The one object 1556+335 has the most stable brightness, the standard deviations are of the order of about of 0.01, similar to the standard deviations of stars. The calculated values of V_C and R_C (input values for differential photometry) magnitudes of stars are in good agreement with V_O and R_O, and the standard deviations of brightness of comparison stars are similar to the ones of control.

In the paper Jovanović (2019) are presented charts of the fields of the objects and their (comparison and control) stars. In paper Jovanović and Damljanović (2020) are presented analysis of objects brightness variability and calculated amplitudes of their quasyperiods form the similar data sets.

Table 2: The coordinates, V and R magnitudes with standard errors of objects and their comparison and control stars; period July 2016 — August 2019.

Object No.	$\alpha_{J2000.0}(^o)$	$\delta_{J2000.0}(^o)$	$V_C \pm \sigma_{V_C}$(mag)	$R_C \pm \sigma_{R_C}$(mag)	$V_O \pm \sigma_{V_O}$(mag)	$R_O \pm \sigma_{R_O}$(mag)
1535+231	234.31041	23.01126			18.375 ±0.197	18.099 ±0.214
2 (A)	234.31491	23.01831	17.200 ± 0.031	16.658 ± 0.038	17.213 ±0.024	16.693 ±0.036
3	234.30004	23.02486	15.983 ± 0.030	15.633 ± 0.031	16.000 ±0.024	15.656 ±0.030
4 (B)	234.25178	23.01917	16.232 ± 0.024	15.867 ± 0.029	16.227 ±0.010	15.851 ±0.017
7	234.29312	22.96096	16.470 ± 0.027	15.973 ± 0.036	16.451 ±0.026	15.958 ±0.021
8	234.35917	23.01592	15.860 ± 0.035	15.149 ± 0.050	15.841 ±0.024	15.142 ±0.028
1556+335	239.72993	33.38851			17.501 ±0.048	17.020 ±0.040
2 (A)	239.71950	33.39110	17.336 ± 0.030	16.850 ± 0.038	17.344 ±0.031	16.895 ±0.032
3 (B)	239.69035	33.40959	16.381 ± 0.027	16.095 ± 0.030	16.378 ±0.013	16.074 ±0.015
5	239.76798	33.38778	16.271 ± 0.030	15.916 ± 0.031	16.289 ±0.025	15.936 ±0.023
6	239.74562	33.39003	16.198 ± 0.030	15.825 ± 0.031	16.225 ±0.022	15.876 ±0.021
7	239.74317	33.37370	15.552 ± 0.030	15.188 ± 0.031	15.568 ±0.022	15.223 ±0.017
8	239.73398	33.37219	15.743 ± 0.040	14.897 ± 0.064	15.756 ±0.045	14.966 ±0.016
1607+604	242.08560	60.30783			17.461 ±0.104	17.000 ±0.084
2 (A)	242.02882	60.28951	17.068 ± 0.027	16.619 ± 0.031	17.057 ±0.015	16.601 ±0.017
3 (B)	242.02526	60.31162	16.864 ± 0.025	16.423 ± 0.032	16.874 ±0.013	16.439 ±0.015
4	241.97352	60.35552	15.195 ± 0.025	14.781 ± 0.031	15.164 ±0.059	14.715 ±0.050
5	242.09638	60.34816	15.630 ± 0.031	14.965 ± 0.044	15.601 ±0.041	14.929 ±0.036
7	242.16854	60.37746	16.856 ± 0.024	16.467 ± 0.031	16.838 ±0.050	16.389 ±0.061
1722+119	261.26810	11.87096			15.540 ±0.633	15.013 ±0.613
C2	261.27167	11.86997	13.173 ± 0.005	12.570 ± 0.006	13.177 ±0.019	12.628 ±0.025
C3	261.24375	11.86636	14.078 ± 0.012	13.600 ± 0.008	14.082 ±0.020	13.629 ±0.015
1	261.31208	11.89125	13.445 ± 0.009	12.848 ± 0.010	13.440 ±0.024	12.857 ±0.024
2 (A)	261.30458	11.86519	14.823 ± 0.008	14.691 ± 0.012	14.829 ±0.008	14.688 ±0.005
5	261.25667	11.91311	15.873 ± 0.010	15.385 ± 0.016	15.857 ±0.043	15.378 ±0.022
9	261.23333	11.87083	15.809 ± 0.008	15.332 ± 0.014	15.799 ±0.019	15.339 ±0.018
10	261.23875	11.87083	16.142 ± 0.011	15.699 ± 0.019	16.134 ±0.013	15.712 ±0.020
C4 (B)	261.28958	11.85344	15.665 ± 0.009	15.164 ± 0.013	15.653 ±0.017	15.169 ±0.007
1741+597	265.63334	59.75186			17.945 ±0.372	17.545 ±0.376
2	265.62329	59.75176	15.565 ± 0.029	15.204 ± 0.054	15.619 ±0.032	15.290 ±0.042
3 (A)	265.57081	59.75387	16.673 ± 0.029	16.314 ± 0.053	16.678 ±0.014	16.331 ±0.015
4	265.68412	59.76861	16.376 ± 0.034	15.795 ± 0.067	16.407 ±0.029	15.840 ±0.024
5	265.61457	59.79547	16.154 ± 0.031	15.704 ± 0.056	16.187 ±0.040	15.753 ±0.024
6	265.68288	59.71901	16.126 ± 0.038	15.684 ± 0.064	16.137 ±0.023	15.696 ±0.022
7 (B)	265.59766	59.71686	16.633 ± 0.039	16.124 ± 0.074	16.629 ±0.013	16.110 ±0.012

Note. (A), (B) refer to comparison stars.

3. METHODS AND RESULTS

Some of the data were rejected after applying 3-σ rule. After implementation of Shapiro-Wilk test of normality we conclude that statistical tests which require normal data distribution can be applied.

3.1 F-test

We used the F-test to investigate the brightness variability of objects (de Diego 2010, Gupta et al. 2017, Jovanović 2019), by comparing variances of two data sets. The test statistic are:

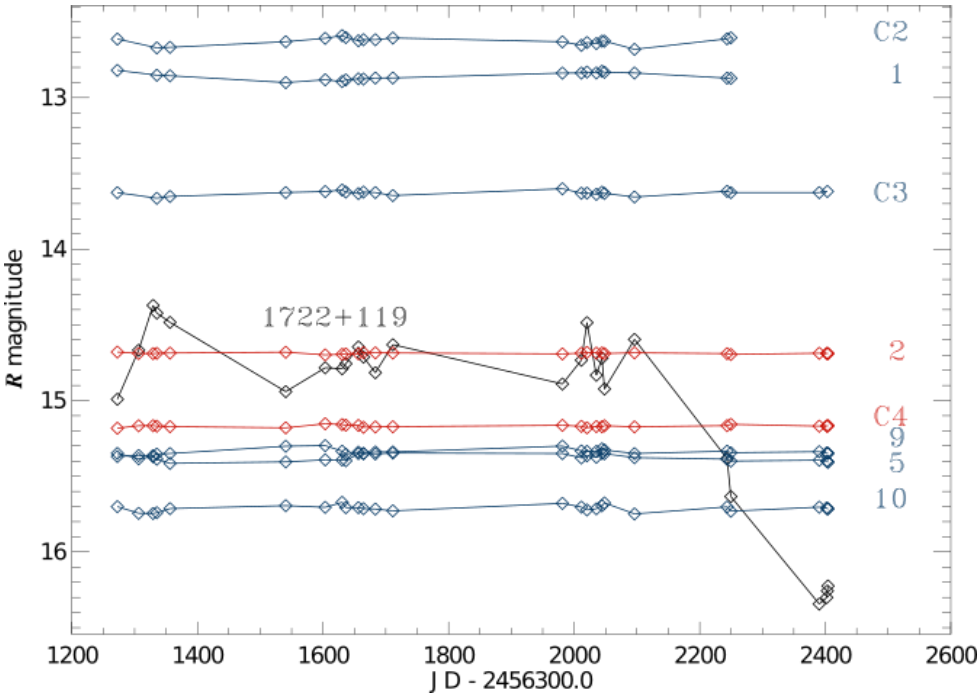

Figure 1: The light curve of R magnitude of 1722+119 and light curves of its comparison and control stars, from July 2016 until August 2019.

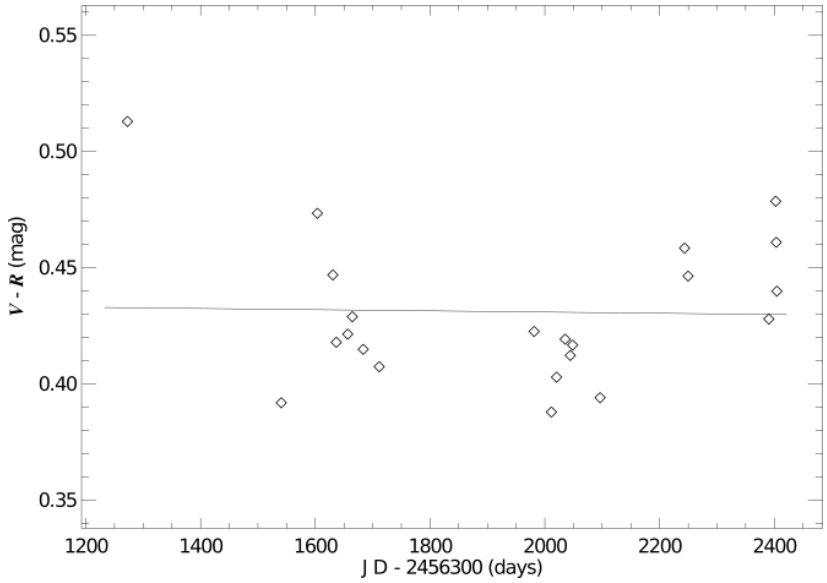

Figure 2: The light curve of color indices V-R variability during period July 2016 – August 2019, of object 1722+119.

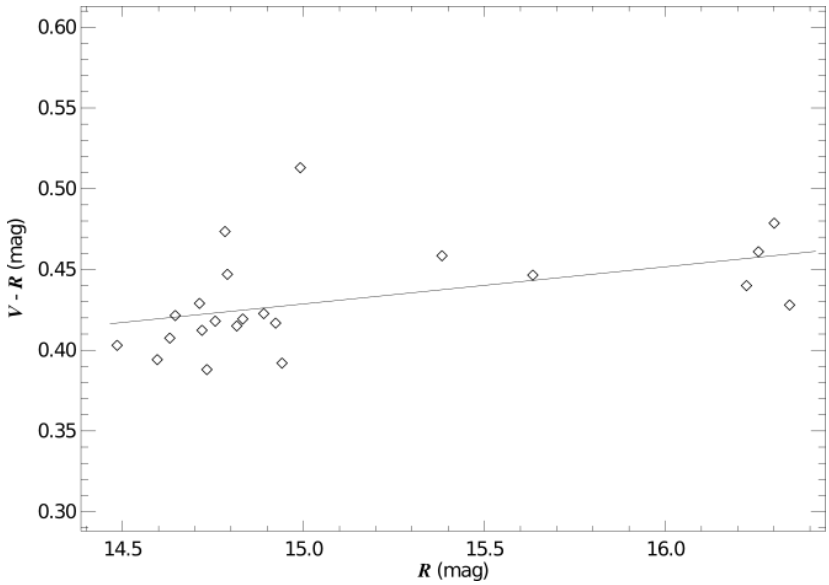

Figure 3: The correlation between color indices V-R and R-band magnitude, of object 1722+119.

$$F_1 = \frac{VAR(O-A)}{VAR(O-B)}\,, \quad F_1 = \frac{VAR(O-A)}{VAR(A-B)} \quad \text{and} \quad F_1 = \frac{VAR(O-B)}{VAR(A-B)}\,.$$

The designations O − A, O − B, and A − B refer to the differences of obtained magnitudes of object (O) and comparison star A, object and comparison star B, and comparison star A and B, respectively. The brightness of control stars was investigate by using the same test statistics (O refers to the magnitude of the control star). The variances VAR(O-A), VAR(O-B) and VAR(A-B) are the variances of mentioned differences.

The F_i (i=1, 2, 3) statistics were compared with critical values. The F_1 value should be around 1, because it is expected that the variances VAR(O-A) and VAR(O-B) should be close to each other. Tested brightness should be variable in the same manner for both comparison stars (A and B). When the F_2 and F_3 values are greater then critical (which correspond to the significance level 0.05 and number of freedom N-1, where N is the number of data), the null hypothesis (non variability) is discarded.

Results of F-test are different from in paper Jovanović and Damljanović (2020) because of the changing the selection of comparison stars (1607+604), and after rejecting some CCD images which were obtained during bad atmospheric conditions (1722+119 and 1741+597). The test shows that one object 1556+335 is non variable, the F_i values are almost equal 1, for V (F_1=1.11, F_2=1.34, and F_3=1.49) and R filter (1.23, 1.22, and 1.01). The critical values are 2.17 and 1.93,

for V and R filter respectively. For the four variable objects F_1 values are around 1 as it is expected, but F_2 and F_3 are greater than the critical value. The $F_{2,3}$ values, along with number of data points N, and critical values Fc (for N and $\alpha = 0.05$) are listed in Table 3, for both filters. It is noticeable that the objects with significant brightness variability (1722+119 and 1741+597) have the higher $F_{2,3}$ values. The test shows that the brightness of control stars could be considered as non-variable.

Table 3: The F-test results.

Object	Filter	N	F_2, F_3	F_c
1535+231	V	20	31.39, 36.23	2.17
	R	24	15.08, 17.14	2.01
1607+604	V	23	14.09, 14.10	2.05
	R	27	6.69, 7.02	1.93
1722+119	V	22	621.18, 596.30	2.08
	R	26	2833.73, 2852.28	1.96
1741+597	V	34	190.86, 196.33	1.79
	R	40	183.66, 187.02	1.70

3.2 Color variability

We investigate the color indices V-R variations with respect to time (color vs. time) and with respect to R-band magnitude (color versus magnitude) of the five presented objects (variable and non variable). The data are fitted using Linear Least Squares (LLS) fit (y=a+bx). In addition, the linear Pearson correlation coefficients, r, were calculated

$$r = \frac{\sum(x-\bar{x})(y-\bar{y})}{\sqrt{\sum(x-\bar{x})^2 \sum(y-\bar{y})^2}}$$

where x is the time (color – time dependences) or R magnitude (color – magnitude dependences), y is color, x and y are corresponding average values of data.

The values of the standard errors of the (LLS) fits, intercepts, a, the slopes, b, the linear Pearson correlation coefficients, r, for color vs. time and color vs. magnitude are reported in Tables 4 and 5, respectively.

Table 4: The color variations with respect to time.

Object	σ_0	$a \pm \sigma_a$	$b \pm \sigma_b$	r
1535+231	0.084	0.347 ± 0.111	-5.36E-5 ± 5.88E-5	-0.205
1556+335	0.052	0.496 ± 0.072	-6.63E-6 ± 3.85E-5	-0.039
1607+604	0.067	0.587 ± 0.092	-6.02E-5 ± 4.82E-5	-0.258
1722+119	0.032	0.436 ± 0.041	-2.56E-6 ± 2.06E-5	-0.027
1741+597	0.085	0.649 ± 0.107	-8.41E-5 ± 5.53E-5	-0.260

Note. σ_0 =*stanadrd error*, a = *intercept*, b = *slope* of Color indices against $JD - 2456300$ and r = *Pearson coefficient.*

Table 5: The color – magnitude dependences.

Object	σ_0	$a \pm \sigma_a$	$b \pm \sigma_b$	r
1535+231	0.076	3.468 ± 1.380	-0.178 ± 0.076	-0.472
1556+335	0.047	10.300 ± 4.441	-0.577 ± 0.261	-0.452
1607+604	0.069	-0.788 ± 3.307	0.074 ± 0.195	0.081
1722+119	0.028	0.084 ± 0.148	0.023 ± 0.010	0.456
1741+597	0.085	-0.552 ± 0.743	0.060 ± 0.043	0.240

Note. σ_0 =*stanadrd error*, a = *intercept*, b = *slope* and r = *Pearson coefficient.*

It seems that there are no consistent systematic trends in the color variations, as shown in Table 4 and LLS fits to the color versus time plots (one example is presented in Figure 2). The three BL Lac objects (1607+604, 1722+119, and 1741+597) show bluer when brighter (BWB) trends (Table 5), unlike two objects which are QSO type (1535+231 and 1556+335).

The examples of the color versus time and color versus magnitude plots, of the object 1722+119, are presented in Figure 2 and Figure 3, respectively.

4. CONCLUSIONS

In this paper are presented results of the color variation of five objects (3 BL Lac and 2 QSO) during a period of about 3 years. The calculated V_C and R_C magnitudes (used values for the differential photometry) of all comparison and control stars are in a good agreement with magnitudes which were determined from the observations (V_O and R_O) in line with their standard errors (see Table 2). We applied F–test to investigate brightness variability of objects and their control stars. The test shows that significant changes of brightness variability of stars were not detected, and we consider that they are suitable for photometric measurements. During period July 2016 – August 2019, only one object, 1556+335, did not show brightness variability. In the previously published papers (Jovanović 2019, Jovanović and Damljanović 2020) are presented amplitude of the quasyperiods of four variable objects. In this paper in the Table 3 are presented results of F-test for four variable objects. The two objects with higher differences between maximum and minimum brightness have the higher test statistics than the other objects. For

the five presented objects in Table 4 and Table 5 are listed results of analysis of brightness color variations and color – R magnitude dependences. Two objects of QSO type were found redder when they are brighter trends and for three BL Lac objects bluer when they are brighter (BWB) trends. The BWB trend is a well-observed feature in blazars especially in BL Lac object. To better determine coefficients of fitting and understand physical process and cause of objects variability, we need to continue with observations. It is necessary to proceed with further observations in order to investigate variability of object brightness (the Intra Day and Long Term variability) and color.

Acknowledgements

During the work on this paper authors were financially supported by the Ministry of Education, Science and Technological Development of the Republic of Serbia through the contract No 451-03-68/2020-14/200002. We gratefully acknowledge the observing grant support from the Institute of Astronomy and Rozhen National Astronomical Observatory, Bulgarian Academy of Sciences, via bilateral joint research projects ”Gaia Celestial Reference Frame (CRF) and fast variable astronomical objects”, and “Astrometry and photometry of visual double and multiple stars”.

References

Abolfathi B., Aguado D. S., Aguilar G., et al.: 2018, *Astrophys. J. Suppl. Ser.*, 235, 42.

Bourda G., Collioud A., Charlot P., Porcas R., Garrington S.: 2011, *Astron. Astrophys.*, 526, A102.

Charlot P., Jacobs C. S., Gordon D., et al.: 2020, arXiv e-prints arXiv:2010.13625, 2010.13625.

Chonis T. S., Gaskell C. M.: 2008, *The Astronomical Journal*, 135, 264.

De Diego J. A.: 2010, *Astron. J.*, 139, 1269.

Doroshenko V. T., Efimov Yu. S., Borman G. A., Pulatova N. G.: 2014, *Astrophysics*, 57, 2.

Gaia Collaboration, Brown A. G. A, Vallenari A., Prusti T., et al.: 2018, *A&A*, 616, A1.

Gupta A. C.: 2014, *J. Astrophys. Ast*r., 35, 307.

Gupta A. C., Agarwal A., Mishra A., et al.: 2017, *Mon. Not. R. Astron. Soc.*, 465, 4423.

Jovanović M. D.: 2019, *Serb. Astron. J.*, 199, 55-64.

Jovanović M. D., Damljanović G.: 2020, *Bulg. Astron. J.*, Vol 33, 9pp.

Tody, D.: 1986, *Proceedings SPIE Instrumentation in Astronomy VI*, ed. D.L. Crawford, 627, 733.

Tody, D.: 1993, *Astronomical Data Analysis Software and Systems II, A.S.P. Conference Ser.*, eds. R.J. Hanisch, R.J.V. Brissenden, & J. Barnes, 52, 173.